IOP Publishing and International Atomic Energy Agency Nuclear Fusion

Nucl. Fusion **50** (2010) 025016 (10pp) doi:10.1088/0029-5515/50/2/025016

Investigating behaviours of hydrogen in a tungsten grain boundary by first principles: from dissolution and diffusion to a trapping mechanism

Hong-Bo Zhou[1], Yue-Lin Liu[1], Shuo Jin[1], Ying Zhang[1], G.-N. Luo[2] and Guang-Hong Lu[1]

[1] Department of Physics, Beijing University of Aeronautics and Astronautics, Beijing 100191, People's Republic of China

[2] Institute of Plasma Physics, Chinese Academy of Sciences, Hefei 230031, People's Republic of China

E-mail: LGH@buaa.edu.cn (G.-H. Lu)

Received 24 September 2009, accepted for publication 8 December 2009
Published 15 January 2010
Online at stacks.iop.org/NF/50/025016

Abstract

We have investigated the dissolution, segregation and diffusion of hydrogen (H) in a tungsten (W) grain boundary (GB) using a first-principles method in order to understand the GB trapping mechanism of H. Optimal charge density plays an essential role in such a GB trapping mechanism. Dissolution and segregation of H are directly associated with the optimal charge density, which can be reflected by the H solution and segregation energy sequence for the different interstitial sites. To occupy the optimal-charge-density site, H can be easily trapped by the W GB with the solution and segregation energy of −0.23 eV and −1.11 eV, respectively. Kinetically, such a trapping is easier to realize due to the much lower diffusion barrier of 0.13–0.16 eV from the bulk to the GB in comparison with the segregation energy, suggesting that it is quite difficult for the trapped H to escape out of the GB. However, the GB can hold no more than 2 H atoms because the isosurface of optimal charge density almost disappears with the second H atom in, leading to the conclusion that H_2 molecule and thus H bubble cannot form in the W GB. Taking into account the lower vacancy formation energy in the GB as compared with the bulk, we propose that the experimentally observed H bubble formation in the W GB should be via a vacancy trapping mechanism.

PACS numbers: 61.82.Bg, 67.63.−r, 61.72.Mm, 66.30.J−

(Some figures in this article are in colour only in the electronic version)

1. Introduction

Energy shortage is considered to be the most important problem mankind faces, and nowadays great efforts have been made to develop new kinds of energy resources. One of them is nuclear fusion energy, which is a clean and infinite energy resource for future generation. Fusion energy is being developed internationally via the International Thermonuclear Experimental Reactor (ITER) Project [1], which aims to demonstrate the extended burn of deuterium–tritium (D–T) plasma in a fusion reaction. The mechanical property of plasma facing materials (PFMs) under D–T plasma irradiation is one of the most important issues for the ITER project. The types of damage for the PFMs in a fusion reaction include displacement damage caused by high energy neutrons and surface damage such as blistering, erosion and sputtering caused by helium (He) and hydrogen (H) from the plasma.

High-Z materials are potential candidates for the armour materials of PFMs. Among all the high-Z materials, tungsten (W) and W alloys are regarded as the most promising candidates for PFMs because of their good thermal properties, such as high thermal conductivity, high melting temperature and low sputtering erosion [2]. However, as a PFM, W will be exposed to extremely high fluxes of H isotope ions. It must not only withstand radiation damage, but also keep intrinsic mechanical properties and structural strength. H radiation may change the microstructure and mechanical properties of W.

Generally, defects in materials such as grain boundaries (GBs), dislocations and vacancies are considered to be the origin for H bubble formation in W. The role of GBs gets

much more attention among them. GB is one of the main defects in materials, acting as a transition region between two adjacent crystal lattices, and thus the chemical composition and crystallographic structure of GBs are distinct from those of the bulk crystal. Therefore, such distinct composition and structure powerfully affect the chemical and physical behaviour of GBs, and the properties of materials with GBs can considerably differ from those of a single crystal [3]. Some elements will segregate to the GBs due to the difference in chemical composition between GBs and the surrounding bulk [4]. By using GB engineering, it is possible to improve the mechanical, chemical and magnetic properties of materials significantly [5–8].

Many recent efforts have been devoted to understanding the interaction between H and its isotopes with W. Previous studies [9–14] suggest that W GB plays an important role in the formation of H bubbles. The H bubbles would most possibly form along the W GBs [9]. The implanted H would diffuse further into the material, which could eventually find trapping sites in GBs and collect [10, 11], leading to the nucleation and growth of H bubbles [12, 13]. The formation of H bubbles (blisters) would reduce GB adhesion [13]. On the other hand, GBs can also have effects on the structure and size of H bubbles [14].

Now, it is feasible to employ the first-principles method based on density functional theory (DFT) to determine the interaction between impurities and GBs. The charge-transfer mechanism caused by H segregating at iron GB gives a successful explanation for the historical issue of H embrittlement [15, 16]. Recent first-principles studies [17, 18] show that H prefers to occupy the tetrahedral interstitial site (TIS) in W bulk, and two H atoms interact with an equivalent distance of 2.2 Å. In combination with the molecular dynamics and kinetic Monte Carlo methods [17], it is demonstrated that H cannot be self-trapped in W bulk, which explains the different bubble-formation depth of H from He as observed in the experiment. In our previous work [19], we revealed the microscopic vacancy trapping mechanism for H bubble formation in W bulk based on first-principles calculations of the energetics of H–vacancy interaction and the kinetics of H segregation. Vacancy provides an isosurface of optimal charge density that induces collective H binding on its internal surface, a prerequisite for the formation of H_2 molecule and nucleation of H bubble inside the vacancy.

Previous experimental studies indicate that W GBs are directly associated with the formation of H bubbles. Yet the formation mechanism has not been well understood. So far little work focuses on this aspect. In order to understand the physical mechanism of H trapping and investigate the kinetics of H in the W GB, in this paper, we have systematically investigated the dissolution, segregation, diffusion and trapping mechanism of H in a W GB using the first-principles method. Our calculations will provide a good reference for developing W materials as a PFM.

2. Computational method

We employ a first-principles plane-wave method based on DFT with generalized gradient approximation (GGA) according to Perdew and Wang [20] using the VASP [21–23]. The interaction between ions and electrons is described by the projector augmented wave (PAW) potential based on GGA. It should be mentioned here that the GGA overestimates the lattice constant but underestimates the binding energy as compared with the experimental values, in contrast with the LDA [24, 25]. The energy cutoff for the plane wave basis was chosen to be 350 eV. The supercell contains 80 W atoms to simulate the 36.9° [1 0 0]{0 1 3} $\Sigma = 5$ symmetrical title GB. The calculated equilibrium lattice constant is 3.17 Å for bcc W, in good agreement with the corresponding experimental value of 3.16 Å. The lattice constants for the W GB supercell are 20.87 Å × 9.97 Å × 6.29 Å. For summation over the Brillouin zone, the uniform grids of k-points are 1 × 2 × 3 according to the Monkhorst–Pack scheme with a full relaxation of the atomic positions and volume of the supercell [26]. The energy relaxation iterates until the forces acting on all the atoms are less than 10^{-3} eV Å^{-1}.

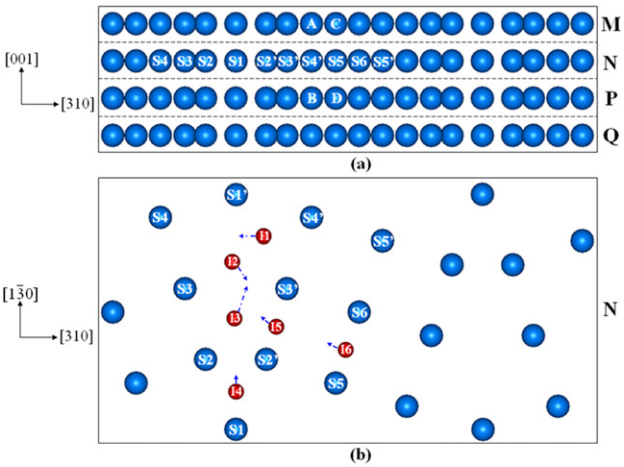

Figure 1. (*a*) Side view of Σ5(310)/[001] tilt W GB. (*b*) Top view of the N atom layer of the W GB supercell. Schematically, the larger blue spheres represent the W atoms, while the smaller red spheres (numbers I1–I6) represent the six different interstitial sites in the N atom layer. Numbers S1–S6 represent the six different substitutional sites of the H substitution for W. W atoms are denoted by S1′– S5′ and A–D are for later discussion. The arrows show the moving directions after structure optimization.

3. Results and discussion

3.1. Dissolution of single H atom in W GB

In order to find the most favourable site of single H atom in the W GB, we examine the solution energies of all potential GB sites for H, including interstitial and substitutional cases. We only consider H in the N atom layer, because the sites that H occupies are symmetrically equivalent for the N and M layers, and the N and M layers are totally the same as the periodical Q and P layers. As shown in figure 1, the H atom has been set up in 12 different sites on the N layer in the GB, in which half (I1–I6) are for the interstitial cases and the other half (S1–S6) are for the substitutional cases. Further, we also consider the vacancy in the GBs with a vacant lattice site for all the substitutional cases (S1–S6). These vacancies are named V1–V6 with the same sequence as the substitutional cases. When H occupies an interstitial site, the solution energy of $E_{\mathrm{I}}^{\mathrm{sol}}$ is

expressed by

$$E_{\mathrm{I}}^{\mathrm{sol}} = E_{\mathrm{W-H}}^{\mathrm{T}} - E_{\mathrm{W}}^{\mathrm{T}} - \tfrac{1}{2}E_{\mathrm{H_2}}, \quad (1)$$

where $E_{\mathrm{W-H}}^{\mathrm{T}}$ and $E_{\mathrm{W}}^{\mathrm{T}}$ are the total energies of the W GB supercell with and without H, respectively. The third term $\frac{1}{2}E_{\mathrm{H_2}}$ is one-half of the energy of a H_2 molecule, which is calculated by putting two H atoms to form the H_2 molecule in a supercell with the side length of ~15 Å. We chose one-half of the energy of the H_2 molecule as the reference energy (−3.38 eV according to the present calculation) so that we can conclude whether the H solution in W is endothermic (the solution energy is positive) or exothermic (the solution energy is negative).

The present energetic results can reasonably be compared with the experiment although the temperature effects are not been taken into account. We take the binding energy as an example. The binding energy is 4.54 eV (with respect to spin-polarized H atoms) for a H_2 molecule with a bond length of 0.75 Å, consistent with the previous GGA results [27]. Importantly, the values agree well with experimental values of 4.75 eV and 0.74 Å [28].

According to equation (1), the solution energy of H at the TIS in W is calculated to be +0.89 eV. It is positive, indicating that the dissolution of H in bulk W is an endothermic process, consistent with the experimental observation [29, 30]. However, the solution energy for H occupying the most stable sites at vacancy is negative with the value of −0.31 eV. This suggests that the dissolution of H at the vacancy or vacancy-related defects is an exothermic process due to the larger binding energy of H with the vacancy (−1.18 eV) [19]. The experimentally observed solution energy of H in W is ~ +0.63 eV [30], which is between those of H at TIS and the vacancy. Not taking temperature effects into account, this qualitatively suggests that most of the H atoms occupy the interstitial sites in the bulk, while only a part of them occupy the vacancy-related defects.

When the H atom replaces a W atom, the solution energy of $E_{\mathrm{S}}^{\mathrm{sol}}$ can be obtained by

$$E_{\mathrm{S}}^{\mathrm{sol}} = E_{\mathrm{W-V-H}}^{\mathrm{T}} - E_{\mathrm{W}}^{\mathrm{T}} + E_{\mathrm{W}} - \tfrac{1}{2}E_{\mathrm{H_2}}, \quad (2)$$

where $E_{\mathrm{W-V-H}}^{\mathrm{T}}$ is the total energy of the W GB supercell with single vacancy and one interstitial H atom, and E_{W} is the energy of a W atom in W bulk. For the vacancy cases, the solution energy of $E_{\mathrm{V}}^{\mathrm{sol}}$ is defined as

$$E_{\mathrm{V}}^{\mathrm{sol}} = E_{\mathrm{W-V-H}}^{\mathrm{T}} - E_{\mathrm{W-V}}^{\mathrm{T}} - \tfrac{1}{2}E_{\mathrm{H_2}}, \quad (3)$$

where $E_{\mathrm{W-V}}^{\mathrm{T}}$ is the total energy of the W GB supercells with single vacancy.

Figure 2 shows the solution energies as a function of occupation sites. Because H moves to the same site after the structure optimization for the I2 and I3 cases shown in figure 1(*b*), the solution energies of these two cases are equivalent (−0.23 eV). As illustrated in figure 2(*a*), this is the lowest solution energy among all the interstitial cases. In the substitutional cases, the solution energy of S2 is much lower than that of other sites, which is due to the fact that the W (S2) atom is the easiest to remove from the W GB (lower vacancy formation energy). Moreover, figure 2(*b*) shows that

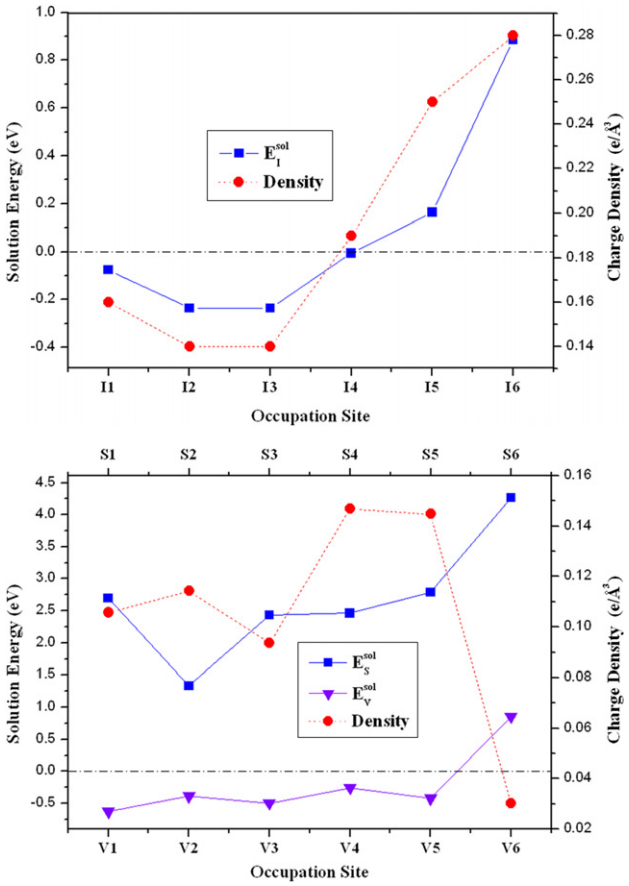

Figure 2. The solution energies and charge densities as a function of different H occupation sites: (*a*) interstitial cases; (*b*) substitutional and vacancy cases. The lines are only to guide the eyes.

the solution energy of the vacancy case is lower in comparison with the substitutional cases. The lowest solution energy is calculated to be −0.63 eV at the V1 site among all the cases.

Physically, the H solution energy (embedding energy) in a metal can be understood approximately in terms of the H solution energy in a homogeneous electron gas [31]. The H solution energy decreases monotonically with decreasing electron density until reaching the minimum at the optimal density of $n_0 \approx 0.018$ electron Å^{-3} (e Å^{-3}) [31]. However, if the charge density is lower than the optimal density, the solution energy increases. With a vacancy in W bulk, H prefers to bind onto an isosurface of the same charge density (0.11 e Å^{-3}) surrounding the vacancy [19]. Since the charge density everywhere in the W GB (as well as in most metals) is much higher than n_0, H generally has the lowest solution energy where the charge density is the lowest.

For the W GB, figure 2(*a*) shows the charge density for the interstitial sites of H after the structure optimization. The solution energy sequence for the optimal interstitial sites of H in the W GB is I2 (I3) < I1 < I4 < I5 < I6. Such a sequence is consistent with the charge density results, i.e. the lower the charge density, the lower is the solution energy. On the other hand, the solution energies for the substitutional cases are much larger than those for the vacancy case as shown in figure 2(*b*). This implies that energetically it is quite difficult for H to replace a W atom in the W GB, similar to H in the

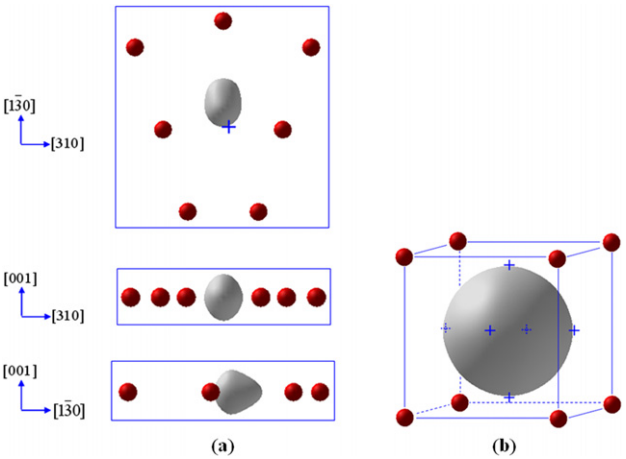

Figure 3. Isosurface of optimal charge density for H binding (*a*) in a W GB and (*b*) at a vacancy in the W bulk. The red (small) balls represent W atoms. The crosses mark the minimum-energy H binding sites on the isosurface in a GB or a vacancy.

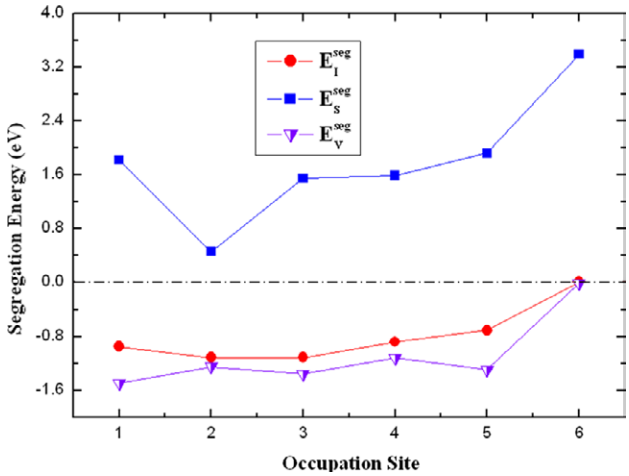

Figure 4. Segregation energies as a function of occupation sites per H atom in a W GB for the interstitial, substitutional and vacancy cases. The lines are only to guide the eyes.

W bulk [17, 18]. The solution energies for the vacancy case decrease with decreasing charge density except for the V6 case. The charge density is ~0.03 e Å^{-3} for V6, much lower than the optimal charge density determined from the first-principles calculation. The solution energy for V6 is thus much higher in comparison with other cases. Since the solution energy for the substitutional case depends on the vacancy formation energy, the charge density for the substitutional cases does not directly correspond to the solution energies. In the substitutional case, the lowest solution energy occurs at the S2 site, because the vacancy formation energy for the S2 site is much lower than that for the other cases with the smallest difference of 1.01 eV.

As mentioned above, in a W GB without vacancy, it is found that single H is energetically favourable sitting at the interstitial site (I2), and binds onto an isosurface of the same charge density (0.14 e Å^{-3}), as shown in figure 3(*a*). While in the W bulk with a monovacancy, H prefers to bind onto an isosurface of the same charge density (0.11 e Å^{-3}) surrounding the vacancy shown in figure 3(*b*) [19]. As a matter of fact, the vacant space in the GB is larger than that a monovacancy provides in the bulk. However, the charge density of the isosurface in the GB is 0.03 e Å^{-3} higher with a smaller isosurface area in comparison with the monovacancy in the bulk. This is because the numbers of W atoms surrounding the vacant space are 13 and 8 for the GB and the monovacancy in the bulk, respectively. The smaller isosurface area in the GB implies the GB can hold fewer H atoms as compared with the monovacancy in the bulk.

As shown in figure 1, the V1, V2 and V3 sites are much closer to the GB. The numbers of W atoms surrounding the V1, V2 and V3 sites are 8, 7 and 8, respectively, quite similar to that of a vacancy in the bulk (8). However, H in the V1, V2 and V3 sites exhibits lower solution energies with lower optimal charge densities as compared with that of the vacancy in the bulk (−0.31 eV). This suggests that the vacancy in the GB can provide a larger isosurface of optimal density than that of the vacancy in the bulk. Consequently, the vacancy in the GB can trap more H atoms than that in the bulk. Furthermore, the H trapping capability of the vacant space that a pure GB provides is lower than that of the vacancy in both the GB and the bulk.

3.2. *Segregation energy of single H atom in a W GB*

In order to show energetically whether H has a tendency to segregate into a W GB, we calculate the segregation energy $E^{\rm seg}(E_{\rm I}^{\rm seg}, E_{\rm S}^{\rm seg}$ and $E_{\rm V}^{\rm seg})$ of H in the W GB. It can be calculated by

$$E^{\rm seg} = \left(E^{\rm T}_{\rm GB,H} - E^{\rm T}_{\rm GB}\right) - \left(E^{\rm T}_{\rm bulk,H} - E^{\rm T}_{\rm bulk}\right), \qquad (4)$$

where $E^{\rm T}_{\rm GB,H}$ and $E^{\rm T}_{\rm GB}$ are the total energies of the W GB system with and without H, and $E^{\rm T}_{\rm bulk,H}$ and $E^{\rm T}_{\rm bulk}$ are the total energies of W bulk system with and without H. For determining $E^{\rm T}_{\rm bulk,H}$ and $E^{\rm T}_{\rm bulk}$, we used the W bulk system crystallizing in the body-centred-cubic structure, which contains 80 atoms with nearly the same size as the corresponding GB system. The lower the segregation energy, the easier the H atom can segregate at the GB.

Figure 4 shows the calculated segregation energies as a function of occupation sites. The sites I1–I5 and V1–V6 in the GB region have a negative segregation energy, while all the substitutional cases have a positive one. This indicates that H favours the interstitial and vacancy cases rather than the substitutional cases in the W GB. The range of the segregation energies for the interstitial cases (I1–I5) is from −0.80 to −1.11 eV, and that for the vacancy cases (V1–V5) is from −1.17 to −1.50 eV. Thus, the GB vacancy site is the most energetically favourable for H segregation. The segregation energies for the vacancy cases are consistent with the experimentally measured binding energies between H and vacancy in W of −1.16 eV [32] and −1.34 eV [33]. This suggests that the experimental value can be associated with the GB vacancies. Furthermore, the range of the segregation energies at V1–V3 is −1.28 to −1.50 eV, much lower than that of the bulk monovacancy (−1.18 eV), suggesting the stronger H-trapping capability of the vacancy in the W GB as compared with the bulk.

Figure 4 also shows that the segregation energy for I6 is zero, indicating the solution energy of H in the I6 site is equal

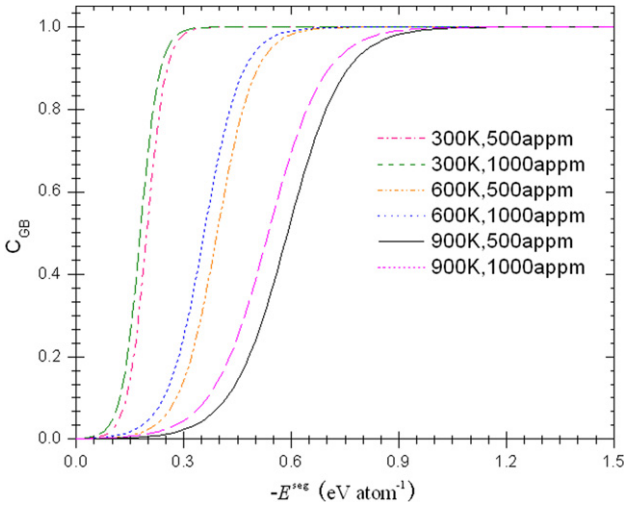

Figure 5. The H concentration in the GB as a function of segregation energy at different temperatures and different bulk H concentrations according to McLean's equation.

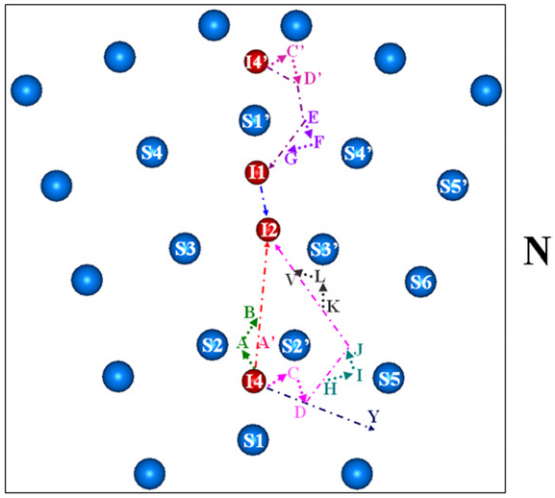

Figure 6. The schematic diffusion paths for H along a W GB, including different I1 → I2, and I4 → I2 paths. The larger blue spheres represent the W atoms, the smaller red spheres represent the stable interstitial sites of H in a W GB after structure optimization. A, C (C′), F, I and L are the interlayer sites between *M* and *N* layers (figure 1), while A′, B, D (D′), E, G, H, J, K, V, Y are the on-layer sites in the *N* layer.

to that of the bulk. Note that the I6 site is at the centre of two GBs, and H at the I6 site occupies the TIS after structure optimization. This suggests that the distance between two GBs in the present simulation supercell is large enough to avoid GB interaction.

From these calculated segregation energies, we can estimate an equilibrium impurity segregation occupation using McLean's equation as follows [34]:

$$C_{GB} = \frac{C_{bulk} \exp(-E^{seg}/RT)}{1 + C_{bulk} \exp(-E^{seg}/RT)}, \quad (5)$$

where E^{seg} is the segregation energy, T is the ageing temperature, R is the molar gas constant, and C_{GB} and C_{bulk} are the occupation of impurity in the GB and the bulk, respectively. When E^{seg} is zero (and/or T is infinitely high), the impurity atoms have the same probability to be in the bulk and the GB; thus the impurity occupation (concentration) in the bulk and the GB will be same ($C_{GB} = C_{bulk}$) due to the fact that C_{bulk} is much smaller than 1. When $E^{seg} < 0$, $C_{GB} > C_{bulk}$ according to McLean's equation, and thus the impurity atom prefers to segregate in the GBs. When $E^{seg} > 0$, $C_{GB} < C_{bulk}$, and the impurity atom prefers to stay in the bulk instead of the GBs. Recent investigations of irradiation of H isotope ions on W [35–41] have clearly shown W surface blistering from room temperature to ~900 K. We thus chose the typical temperature range of 300–900 K and H concentration of 500–1000 atomic parts per million (appm). Figure 5 shows McLean's curves for these temperatures and bulk H concentrations. Clearly, the H GB occupation strongly depends on the temperature, the H concentration in the bulk and the segregation energy. The lower the temperature, the higher the bulk H concentration and the lower the segregation energy, the more H atom can segregate to the GB. In the ranges 300–900 K and 500–1000 appm, the segregation energy plays an important role in the H GB segregation. In these ranges, segregation energy lower than −1.0 eV will lead to the segregation of all the H atoms to the GB, independent of the temperature and concentration. As illustrated in figure 4, the segregation energies of H occupying the vacancy site and the most stable interstitial site in the GB are lower than −1.0 eV. Consequently, almost all the H atoms will segregate in the W GB in the above temperature and concentration ranges.

3.3. Migration of H along a W GB

Understanding the diffusion properties of H will provide a good reference for H clustering and thus H bubble formation in the W GB. There are two main mechanisms for impurity atoms diffusing in a solid, i.e. the interstitial and substitutional mechanisms, which depend on the occupation behaviour of the impurity atoms. The H atom has been demonstrated to occupy the interstitial sites in W [17, 18]. Therefore, H will diffuse in W via the interstitial mechanism. Here, we determine the diffusion energy barrier of H in the W GB using a drag method at a fixed volume and constraining the atomic position to relax in a hyperplane perpendicular to the vector from the initial to final positions [42].

In order to investigate the diffusion properties of H along the W GB, we choose three typical sites in the GB, i.e. I1, I2 and I4. I2 has been shown to be the most energetically favourable site for H to segregate in the GB, while I1 and I4 are the metastable sites, as illustrated in figure 2(*a*). As shown in figure 1, the structures are symmetrically equivalent for the *N* and *M* atom layers, and the *N* and *M* layers are totally the same as the periodical *Q* and *P* layers. Therefore, the diffusion behaviour of H in the *N* atom layer is able to cover all other cases. To seek the optimal diffusion path for both I1 → I2 and I4 → I2, we calculate diffusion energy profiles for the chosen different paths, as shown in figure 6.

As shown in figure 7(*a*), the H atom jumps from the metastable site I1 to the most stable site I2 with a diffusion energy barrier of 0.13 eV, which is lower than that of H in the W bulk by 0.07 eV. In the W bulk, H diffuses between the TIS sites via an interstitial mechanism with the energy barrier of

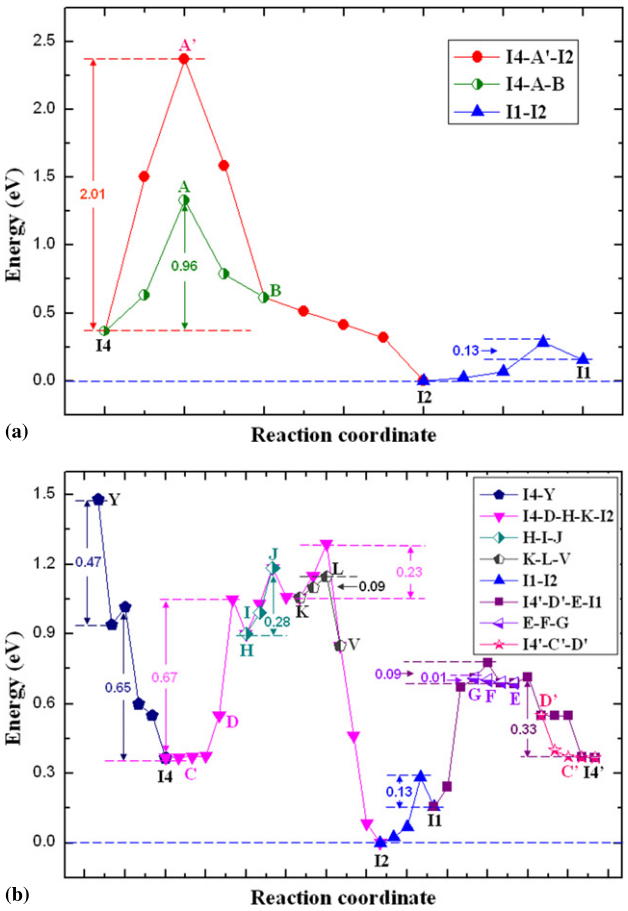

Figure 7. Diffusion energy profiles for H migrating from I1 and I4 to I2 along the W GB. Letters and numbers correspond to those in figure 6.

0.20 eV [18]. This indicates that the H atom at the I1 site will easily jump to the I2 site.

For the diffusion from another metastable site I4 to I2, we first consider the diffusion path directly along the GB. The diffusion energy barrier for H jumping from I4 to I2 through A′ along the W GB is 2.01 eV, much larger than that for the I1 → I2 path. The transition state occurs at the middle site A′ between S2 and S2′, as shown in figure 6. Such a higher barrier should originate from the shorter distance between S2 and S2′ due to the presence of GB, which is only 2.57 Å, much shorter than the lattice constant of the W bulk (3.17 Å). Consequently, the charge density is 0.5 e Å^{-3} at the middle site between S2 and S2′, which is much higher. However, the energy barrier of 2.01 eV can be significantly lowered to 0.96 eV if H diffuses via the path I4 → A → B → I2, but the barrier is still much higher than that for the I1 → I2 path. The transition state for I4 → A → B → I2 occurs at the middle site between S2 and S2′ but above the *N* layer (A). Despite the much lower barrier (0.96 eV) as compared with that for the I4 → A′ → I2 path, it is still much higher than the barrier for H diffusion in the bulk (0.20 eV). Further, such a barrier is also higher than the segregation energy of I4 by 0.08 eV. This implies that I4 → A → B → I2 should not be the optimal path.

We thus next seek other potential paths that are not directly along the GB. Three paths are attempted. Via the first path, I4 jumps towards the bulk through an octahedral-like interstitial site to Y site, and finally returns to I2 at the GB from the bulk. The energy barrier for this path should be ∼0.65 eV, as shown in figure 7(*b*).

The second path is I4 → H → K → I2 close to the GB. Along the second path, H diffuses along several processes, including I4 → D → H, H → I → J → K and K → L → V → I2, the energy barriers for which are 0.67 eV, 0.28 eV and 0.23 eV (0.09 eV), respectively (figure 7(*b*)). Therefore, the diffusion energy barrier is 0.67 eV for the second path, approximately the same as that for the first path.

According to the periodicity of the GB, I4′, C′ and D′ represent the same sites as I4, C and D in the next period, respectively, as shown in figure 6. Let H in the I4′ site first go to I1 via the I4′ → D′ → E → G → I1 path and then jump to I2, which is set as the third path. H diffuses through the I4′ → D′ → E, E → G → I1 and I1 → I2 processes, the energy barriers for which are 0.33 eV, 0.09 eV (0.01 eV) and 0.13 eV, respectively (figure 7(*b*)). Therefore, the diffusion energy barrier for the third path is 0.33 eV. Such a barrier is much lower than that for the first and second path, and is the lowest for H jumping for I4 → I2 among all the paths examined.

Clearly, it is much easier for H to diffuse within the vacant space where I2 stays at the GB in comparison with the diffusion from the S1–S2–S2′ triangle region (0.13 versus 0.33 eV). However, the diffusion barriers 0.13 and 0.33 eV are much lower than the H segregation energy in the GB, as illustrated in section 3.2. This suggests that the trapped H should easily aggregate in the GB.

3.4. Migration of H from W bulk to GB

Clearly, the above results demonstrate the thermodynamic feasibility of H GB segregation so as to initiate H bubble formation, as illustrated in section 3.2. Next, we investigate the kinetic process for H jumping from the W bulk to the GB.

As shown in figure 1, the structures are symmetrically equivalent for the *N* and *M* atom layers, and the *N* and *M* layers are totally the same as the periodical *Q* and *P* layers. Therefore, the diffusion behaviour of H in the *N* layer is able to represent all other cases. We examine the diffusion barriers for H jumping to the most stable site I2 at the GB in the *N* layer, for which two symmetrically independent paths have to be taken into account. We name them as paths P1 and P2, in which H has to pass through the S2′–S3′ and S3′–S4′ region, respectively, as shown in figure 8.

For convenience, we mark the representative sites along these two paths. Because H diffusion between the TISs is the optimal path for H in the bulk [18], we consider the TIS-like sites along these two paths for H jumping from the bulk to the GB. Figure 8 shows these sites, and figure 9 shows the structural characteristics of these sites in more detail. Numbers 1–4 at the P1 path and 6–9 at the P2 path are the TIS-like sites. The sites in the *N* layer exactly under the W atoms of A and C are OIS (octahedral interstitial site)-like sites. However, because these regions are closer to the GB, the bond lengths are different from that of bulk (2.75 Å) (figure 9). We can thus predict that the diffusion barrier for H in these regions should be different from that in the bulk.

As reported in the previous studies [18, 43, 44], the diffusion barriers are quite different between the TIS–TIS

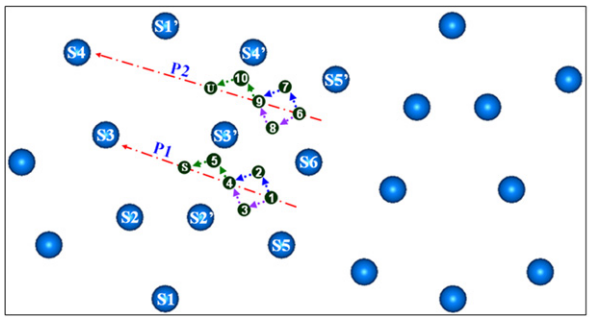

Figure 8. Two representative diffusion paths P1 and P2 for H jumping into a W GB. Sites 1–4 and 6–9 show the TIS-like sites, which are illustrated in figure 9 in more detail. Sites 5 and 10 represent interlayer sites between M and N. The larger blue spheres represent the W atoms. S1–S6 and S1′–S5′ are the same as denoted in figure 1.

(T → T) and TIS–OIS–TIS (T → O → T) paths. The T → T path is calculated to be the optimal diffusion path for H in the bulk W with the energy barrier of 0.20 eV [18]. For the GB case, the diffusion barriers are ∼ 0.20 eV for both T → T paths of 1 → 2 → 4 and 1 → 3 → 4 for the P1 path (figure 10(*a*)), which is much closer to that in the bulk [18]. For the T → O → T path, however, H moves away from the OIS to other more stable sites because the symmetry is destroyed due to the existence of the GB. Such a path exhibits a lower diffusion barrier of 0.13 eV in comparison with the bulk [18]. Then, H goes to the S site with a much lower barrier of 0.09 eV, and reaches the most stable I2 site at the GB barrierlessly (a down-hill 'drift' migration).

For the P2 path (figure 10(*b*)), the diffusion barriers for the T → T paths of 6 → 7 → 9 and 6 → 8 → 9 are 0.20 eV and 0.27 eV, respectively. Obviously, the 6 → 8 → 9 path deviates from the normal T → T path due to the different configurational environment close to the GB, leading to its higher energy barrier. For the T → O → T path, a phenomenon similar to the P1 path occurs. The diffusion barrier is 0.14 eV, lower than that of the T → T path in the bulk. Then H goes to the U site with a much lower barrier of 0.03 eV, and reaches the most stable I2 site at the GB barrierlessly. For both the P1 and P2 paths, the diffusion profiles show the increasing stability of H in the TIS-like site with H approaching the GB.

In addition, there is another path for H to the metastable site I4, for which H has to pass through the S1–S2′ region. This path has been discussed in section 3.3, and the energy barrier for this path (N → 14) is ∼0.16 eV.

The above results demonstrate that kinetically H can easily jump into the GB because the diffusion barrier becomes lower when H approaches the GB. Again, in the case when H jumps into the GB, it is quite difficult to jump out of the GB due to the much lower segregation energy. On the other hand, H in the GB tends to aggregate around the vacant region of the most stable site from the 'energy barrier' point of view.

3.5. H–H interaction in a W GB

Both the H–GB strong binding and the kinetic feasibility suggest that the GB can act as a trapping centre which drives the H atom to segregate towards the GB, which is a necessary prerequisite step for H bubble formation. To investigate this possibility, we examine the interaction of double H atoms in the W GB to find the minimum-energy binding site for the second H. This will make it clear whether H atom can be self-trapped and whether these two H atoms can form a H_2 molecule directly in the W GB.

As discussed above, the interstitial H atom prefers to bind onto an isosurface of optimal charge density (0.14 e Å^{-3}) that a W GB provides, as shown in figure 3(*a*). Further addition of H atoms will lead to a shrinking of the isosurface of optimal charge density so that there will be fewer available optimal-density sites to accommodate additional H atoms, as illustrated in our previous study [19]. Figure 11(*a*) shows a large isosurface shrinkage with one H atom added. Since the optimal density region still exists, we can predict that it is energetically favourable for the GB to trap the second H atom [19, 31]. The cross marked in figure 11(*a*) shows a possible binding site for the second H atom in the W GB.

Despite this, we still choose nine potential sites for the second H atom as shown in figure 12 in order to investigate the energy dependence on the H–H atomic distance. In addition, the configuration effect on the occupation behaviour can also be taken into account. The initial and final H–H distances and the corresponding binding energies are given in table 1. The binding energy E_b between H atoms is defined as

$$E_b = 2E_{1H} - E_{2H} - E_{ref}, \tag{6}$$

where E_{2H} is the energy of the W GB with two H atoms and E_{1H} is the energy of the W GB with one H atom at the most stable interstitial site, while E_{ref} represents the energy of the W GB without H. Obviously, negative binding energy indicates repulsion between H atoms, while positive indicates attraction.

Table 1 shows the largest binding energy to be −0.13 eV for site 2 in figure 12, with the equilibrium distance of 2.15 Å. The binding energy is less than zero, indicating a repulsive H–H interaction in the W GB. In addition, the H–H distance results clearly reflect the configuration effect on the binding energy. An obvious example is for sites 2 and 3, which exhibit equivalent equilibrium distance but with a binding energy difference as large as 0.35 eV. Site 3 has a smaller vacant space and quite different surrounding environment in comparison with site 2.

The binding energy results indicate that the second H atom also prefers to bind onto the isosurface of optimal charge density, which is the same as the first H (figure 11), confirming the above prediction. The isosurface of optimal density almost disappears after the second H atom addition, making a third H atom incapable of finding the available optimal-density site, as shown in figure 11(*b*). This indicates that the GB, despite its larger vacant space, can hold only two H atoms, far fewer than that of the vacancy in the bulk, which can hold as many as ten H atoms [19]. The H–H equilibrium distance for site 2 (2.15 Å, table 1) is much larger than that in a H_2 molecule (0.75 Å according to the present calculation). Hence, H_2 molecule cannot form in a W GB.

However, the previous experiment studies [9–12] reveal that W GBs play an important role in H bubble formation. The implanted H can diffuse further into the material, which could eventually find trapping sites in the GBs and collect, leading to the nucleation and growth of H bubbles. Therefore,

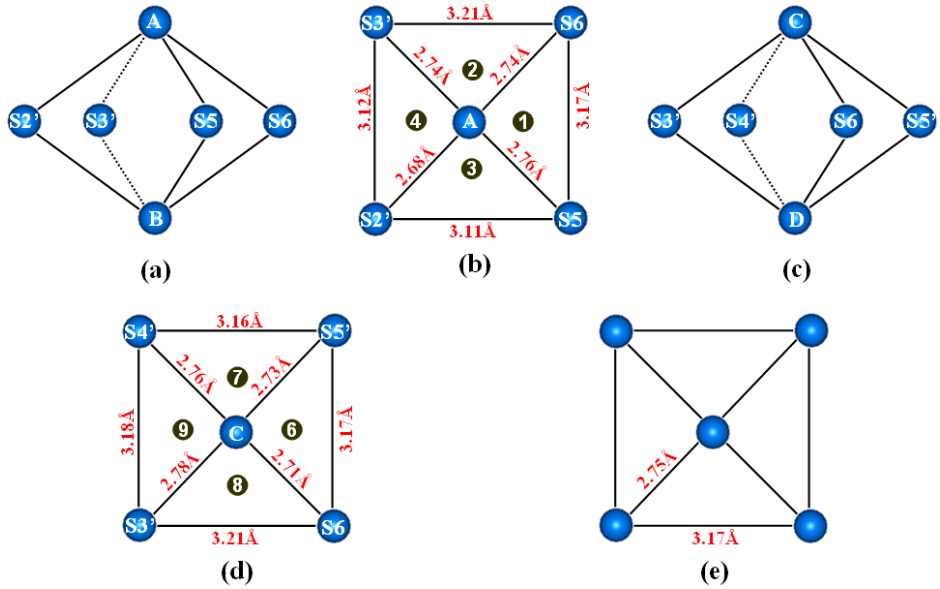

Figure 9. Detailed structural characteristics along the P1 and P2 paths. The letters and the numbers correspond to those in figure 8. (*a*) and (*c*) display the side views, while (*b*) and (*d*) display the top views. (*e*) is the top view of a unit cell in the W bulk for comparison.

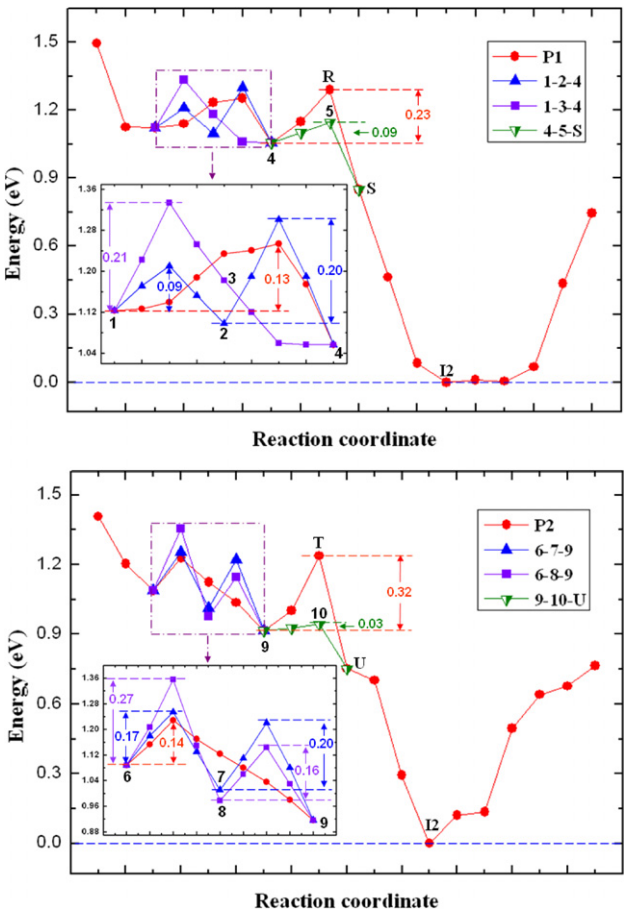

Figure 10. Diffusion energy profile for H jumping into the GB. Letters and numbers correspond to those in figure 8.

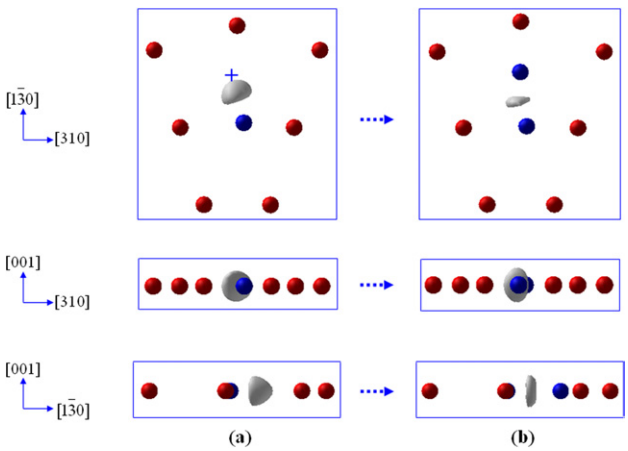

Figure 11. Isosurface of optimal charge density for H binding in a W GB: (*a*) one H atom, (*b*) two H atoms. The cross marks the possible H binding site on the isosurface.

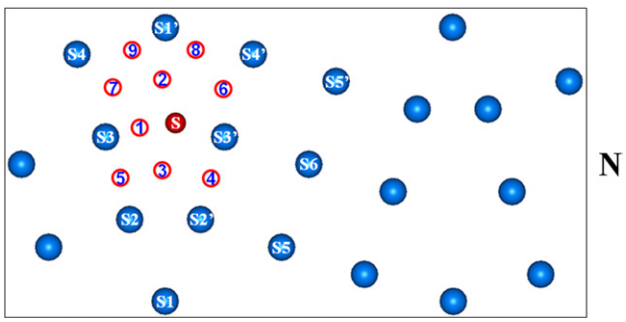

Figure 12. Sites 1–9 represent the possible sites for the second H atom in the GB. The smaller red sphere (S) represents the most stable site for the first H. The larger blue spheres represent the W atoms. The sites S1–S6 and S1′–S5′ denoted in the figure are the same as in figure 1.

to assist the H bubble formation in the W GB, the vacancy or vacancy-like defects should be introduced according to the trapping mechanism in terms of an optimal charge density [19]. Further calculations give the vacancy formation energy in the

Table 1. Initial and final distances (before and after the relaxation, in Å) between two H atoms and the corresponding binding energies (in eV).

Site	Initial distance	Final distance	Binding energy
1	1.23	1.56	−0.31
2	1.34	2.15	−0.13
3	1.69	2.15	−0.48
4	2.25	2.90	−1.05
5	2.61	2.48	−0.47
6	2.78	1.67	−0.24
7	2.97	1.67	−0.23
8	3.12	2.97	−0.64
9	3.37	3.16	−0.64

W GB, which is 1.72 eV. This value is 1.39 eV lower than that in the bulk, which is 3.11 eV [18, 45]. This implies vacancy formation is much easier in the GB as compared with the bulk. We note that the vacancy formation energy in the W bulk is lower than the experimental value of 3.1–4.1 eV [46–48] mainly because of the temperature effect that is not considered in the calculation. Also, H prefers to occupy the vacancy in the GB rather than in the bulk, as illustrated in section 3.1. We thus suggest that the H bubble formation in the W GB should be via a vacancy trapping mechanism.

4. Conclusions

We have investigated the dissolution, segregation and diffusion of hydrogen (H) in a tungsten (W) GB using a first-principles method in order to understand the GB trapping mechanism of H. We show that single H atom energetically prefers to occupy the interstitial site in comparison with the substitutional site in the GB. Dissolution and segregation of H are directly associated with the optimal charge density. Namely, either increasing or reducing the charge density can lead to an energy increase, which can be reflected by the H solution and segregation energy sequence for the different interstitial sites. We found that the W GB can act as a trapping centre for H, comparable to the monovacancy in the W bulk, because the most stable site exists at the vacant space in the GB with the lowest solution and segregation energy, which are −0.23 eV and −1.11 eV, respectively. Such a segregation energy is shown to be low enough for the trapping of almost all H into the GB, independent of the temperature (300–900 K) and the bulk H concentration (500–1000 appm).

Kinetically, we demonstrate the kinetic feasibility of H trapping in the GB so as to initiate H bubble formation. We show that the diffusion barrier for H becomes lower when it approaches the GB, which is in the range 0.13–0.16 eV with one-atomic layer separation from the GB centre. This suggests that, in the case when H jumps into the GB, it is quite difficult to escape out of the GB due to the much lower segregation energy. On the other hand, we found that the diffusion barrier for H diffusion within the GB vacant space is 0.13 eV, lower than that in the bulk (0.20 eV). Such a barrier increases to 0.33 eV from a metastable GB site outside the vacant space. However, both barriers are much lower than the H segregation energy, suggesting the trapped H should easily aggregate in the GB.

Despite its bulk-vacancy-comparable trapping energy, the GB vacant space cannot hold more H atoms because its optimal charge density is 0.14 e Å^{-3}, higher than 0.11 e Å^{-3} for the bulk vacancy. This has been confirmed by the embedding of an additional H atom in the GB vacant space. The isosurface of optimal charge density almost disappears with the second H atom added, making more H atoms incapable of finding their available optimal-charge-density sites. We conclude that H_2 molecule and thus H bubble cannot form in the W GB because the H–H equilibrium distance is 2.15 Å, much larger than that in a H_2 molecule. We propose that, due to the much lower vacancy formation energy in the GB in comparison with the bulk, the experimentally observed H bubble formation in the W GB should be via a vacancy trapping mechanism.

Acknowledgments

This research is supported by the Chinese National Fusion Project for ITER with Grant No 2009GB106003 and the National Natural Science Foundation of China (NSFC) with Grant No 50871009.

References

[1] Causey R., Wilson K., Venhaus T. and Wampler W.R. 1999 *J. Nucl. Mater.* **266–269** 467
[2] Lee H.T., Haasz A.A., Davis J.W. and Macaulay-Newcombe R.G. 2007 *J. Nucl. Mater.* **360** 196
[3] Lejcek P. and Hofmann S. 1995 *Crit. Rev. Solid State Mater. Sci.* **20** 1
[4] Briant C.L. and Messmer R.P. 1982 *J. Phys.* **43** 255
[5] Watanabe T. 1984 *Res. Mech.* **11** 47
[6] Lin P., Palumbo G., Erb U. and Aust K.T. 1995 *Scr. Metall. Mater.* **33** 1387
[7] Randle V. 1999 *Acta Mater.* **47** 4187
[8] Randle V. 2004 *Acta Mater.* **52** 4067
[9] Haasz A.A., Poon M. and Davis J.W. 1999 *J. Nucl. Mater.* **266–269** 520
[10] Causey R.A. 2002 *J. Nucl. Mater.* **300** 91
[11] Shimada T., Kurishita H., Ueda Y., Sagara A. and Nishikawa M. 2003 *J. Nucl. Mater.* **313–316** 204
[12] Funabiki T., Shimada T., Ueda Y. and Nishikawa M. 2004 *J. Nucl. Mater.* **329–333** 780
[13] Ueda Y., Funabiki T., Shimada T., Fukumoto K., Kurishita H. and Nishikawa M. 2005 *J. Nucl. Mater.* **337–339** 1010
[14] Enomoto N., Muto S., Tanabe T., Davis J.W. and Haasz A.A. 2009 *J. Nucl. Mater.* **385** 606
[15] Zhong L.P., Wu R.Q., Freeman A.J. and Olson G.B. 2000 *Phys. Rev.* B **62** 13938
[16] Gesari S.B., Pronsato M.E. and Juan A. 2002 *Appl. Surf. Sci.* **187** 207
[17] Henriksson K.O.E., Nordlund K., Krasheninnikov A. and Keinonen J. 2005 *Appl. Phys. Lett.* **87** 163113
[18] Liu Y.L., Zhang Y., Luo G.N. and Lu G.H. 2009 *J. Nucl. Mater.* **390–391** 1032
[19] Liu Y.L., Zhang Y., Zhou H.B., Lu G.H., Liu F. and Luo G.N. 2009 *Phys. Rev.* B **79** 172103
[20] Perdew J.P. and Wang Y. 1992 *Phys. Rev.* B **45** 13244
[21] Kresse G. and Hafner J. 1993 *Phys. Rev.* B **47** 558
[22] Kresse G. and Furthmüller J. 1996 *Phys. Rev.* B **54** 11169
[23] Kresse G. and Furthmüller J. 1996 *Comput. Mater. Sci.* **6** 15
[24] Zhao Y. and Truhlar D.G. 2004 *J. Phys. Chem.* A **108** 6908
[25] Wong B.M. 2009 *J. Comput. Chem.* **30** 51
[26] Monkhorst H.J. and Pack J.D. 1976 *Phys. Rev.* B **13** 5188
[27] Kresse G. and Hafner J. 2000 *Surf. Sci.* **459** 287
[28] Huber K.P. and Hertzberg G. 1979 *Molecular Spectra and Molecular Structure IV: Constants of Diatomic Molecules* (New York: Van Nostrand Reinhold)

[29] Serra E., Benamati G. and Ogorodnikova O.V. 1998 *J. Nucl. Mater.* **255** 105
[30] Wipf H. 2001 *Phys. Scr.* T **94** 43
[31] Puska M.J., Nieminen R.M. and Manninen M. 1981 *Phys. Rev.* B **24** 3037
[32] Fransens J.R., Keriem M.S.A.E. and Pleiter F. 1991 *J. Phys.: Condens. Matter* **3** 9871
[33] Poon M., Haasz A.A. and Davis J.W. 2008 *J. Nucl. Mater.* **374** 390
[34] McLean D. 1957 *Grain Boundaries in Metals* (London: Oxford University Press)
[35] Sze F.C., Doerner R.P. and Luckhardt S. 1999 *J. Nucl. Mater.* **264** 89
[36] Venhaus T., Causey R., Doerner R. and Abeln T. 2001 *J. Nucl. Mater.* **290–293** 505
[37] Wang W., Roth J., Lindig S. and Wu C.H. 2001 *J. Nucl. Mater.* **299** 124
[38] Tokunaga K., Doerner R.P., Seraydarian R., Noda N., Yoshida N., Sogabe T., Kato T. and Schedler B. 2002 *J. Nucl. Mater.* **307–311** 126
[39] Ye M.Y., Kanehara H., Fukuta S., Ohno N. and Takamura S. 2003 *J. Nucl. Mater.* **313–316** 72
[40] Luo G.N., Shu W.M. and Nishi M. 2005 *J. Nucl. Mater.* **347** 111
[41] Lee H.T., Haasz A.A., Davis J.W., Macaulay-Newcombe R.G., Whyte D.G. and Wright G.M. 2007 *J. Nucl. Mater.* **363–365** 898
[42] Fu C.C., Willaime F. and Ordejon P. 2004 *Phys. Rev. Lett.* **92** 175503
[43] Jiang D.E. and Carter E.A. 2003 *Phys. Rev.* B **67** 214103
[44] Jiang D.E. and Carter E.A. 2004 *Phys. Rev.* B **70** 064102
[45] Becquart C.S. and Domain C. 2007 *Nucl. Instrum. Methods Phys. Res.* B **255** 23
[46] Maier K., Peo M., Saile B., Schaefer H.E. and Seeger A. 1979 *Phil. Mag.* A **40** 701
[47] Wollenberger H. J. 1983 Point defects *Physical Metallurgy* 3rd and enlarged edn ed R.W. Cahn and P. Haasen (Amsterdam: Elsevier Science Publisher BV) chapter 7
[48] Ehrhart P. *et al* 1991 *Atomic Defects in Metals* ed H. Ullmaier (*Landolt-Börnstein New Series* 25) (Berlin: Springer) p 181